



## Experiment Report Form

The double page inside this form is to be filled in by all users or groups of users who have had access to beam time for measurements at the ESRF.

Once completed, the report should be submitted electronically to the User Office using the Electronic Report Submission Application:

<http://193.49.43.2:8080/smis/servlet/UserUtils?start>

### *Reports supporting requests for additional beam time*

Reports can now be submitted independently of new proposals – it is necessary simply to indicate the number of the report(s) supporting a new proposal on the proposal form.

The Review Committees reserve the right to reject new proposals from groups who have not reported on the use of beam time allocated previously.

### *Reports on experiments relating to long term projects*

Proposers awarded beam time for a long term project are required to submit an interim report at the end of each year, irrespective of the number of shifts of beam time they have used.

### *Published papers*

All users must give proper credit to ESRF staff members and proper mention to ESRF facilities which were essential for the results described in any ensuing publication. Further, they are obliged to send to the Joint ESRF/ ILL library the complete reference and the abstract of all papers appearing in print, and resulting from the use of the ESRF.

Should you wish to make more general comments on the experiment, please note them on the User Evaluation Form, and send both the Report and the Evaluation Form to the User Office.


### Deadlines for submission of Experimental Reports

- 1st March for experiments carried out up until June of the previous year;
- 1st September for experiments carried out up until January of the same year.

### Instructions for preparing your Report

- fill in a separate form for each project or series of measurements.
- type your report, in English.
- include the reference number of the proposal to which the report refers.
- make sure that the text, tables and figures fit into the space available.
- if your work is published or is in press, you may prefer to paste in the abstract, and add full reference details. If the abstract is in a language other than English, please include an English translation.



	Experiment title: Structural study of ion-implanted rare-earth species in sol-gel glassy films by EXAFS spectroscopy	Experiment number: 08-01-704
	Beamline: BM08	Date of experiment: from: 20 April 2005 to: 26 April 2005
Shifts: 18	Local contact(s): Dr. Francesco D'ACAPITO (e-mail: dacapito@esrf.fr)	<i>Received at ESRF:</i>
Names and affiliations of applicants (* indicates experimentalists): Dr. Francesco D'ACAPITO*, Prof. Rui M. ALMEIDA*, Prof. Maria Clara GONCALVES, Eng Ana MARQUES*, Dra. Ana RAMOS, Prof. Luís F. SANTOS*		

### Report:

Thin films (thickness of ~300 nm) were prepared by the sol-gel spin-coating method onto silica glass disk substrates (matrix composition:  $\text{SiO}_2\text{-TiO}_2$ ,  $\text{SiO}_2\text{-TiO}_2\text{-HfO}_2$ ,  $\text{SiO}_2\text{-HfO}_2$ ), where Er, Ag and/or Yb are incorporated by ion implantation. Two sol-gel based bulk silica samples, where Ag and/or Er were incorporated by pore-doping, instead of ion implantation, were also analyzed (Sample A10 is doped with Er and sample A11 is doped with Er and Ag).

The photoluminescence (PL) at ~1.54  $\mu\text{m}$  was measured for all samples, heat treated at 900° C after implantation; however its signal is not very intense, probably due to the small thickness of the films. UV/Vis absorption was performed on samples containing silver.

### Experimental conditions:

Extended X-ray absorption fine structure (EXAFS) measurements were performed in grazing incidence geometry, in a dedicated experimental chamber operative at the GILDA-CRG beamline (ESRF beamline BM08), in fluorescence mode, at 6 GeV, at room temperature, by using a Si (111) monochromator and a 13-elements high purity Ge detector. The spectra were recorded from 8100 to 9200 eV. An  $\text{Er}_2\text{O}_3$  compound powder was used as reference standard (obtained in transmission mode). The  $\text{Er}_2\text{Ti}_2\text{O}_7$  and  $\text{Er}_2\text{Si}_2\text{O}_7$  compounds were also taken into account at the fitting procedure.

### L<sub>III</sub> Er-edge measurements with grazing incidence in fluorescence mode:

For all samples, the average position of the first peak (ca. 1.90 Å, without correction for the phase shift) appears similar to that of  $\text{Er}_2\text{O}_3$ , for which the first atomic polyhedron consists of six oxygen neighbors at an average value of 2.26 Å. Thus, we can conclude that the erbium species are present as  $\text{Er}^{3+}$  cations involved in Er-O bonds, since the first neighbor distance in metallic erbium is larger than 3 Å [9].

(The model employed for the fitting procedure considers that the coordination number of Er-Si is the same as the CN of Er-O. Also, the fit was done in K space,  $k^2$ , 2.0-7.7)

Below are some results and conclusions derived from this work:

1. Same results with different grazing incidence angles were obtained, which indicate that the  $\text{Er}^{3+}$  ion environment remains similar as a function of film depth.

2. Different Er contents, as well as the presence of Yb, did not appear to modify the local structure around Er. In fact, its first neighbor was always found to be oxygen (CN~6,  $r \sim 2.27 \text{ \AA}$ ,  $\sigma \sim 0.015$ ). Second neighbor fitting always resulted in Er-O-Si bondings (CN~6,  $r \sim 3.58$ ,  $\sigma \sim 0.02$ ).
3. The presence of ionic and metallic silver had no noticeable effect on the  $\text{Er}^{3+}$  surroundings, regarding first and second neighbors ( $\text{CN}_{\text{oxyg}}=6$ ,  $r=2.28 \text{ \AA}$ ,  $\sigma \sim 0.015$  and  $\text{CN}_{\text{Si}}=6$ ,  $r=3.58$ ,  $\sigma \sim 0.02$ ).
4. The  $\text{Er}^{3+}$  environment was similar in all matrices analyzed: silica-titania (ST), silica-hafnia (SH) and silica-titania-hafnia (STH), when the heat treatment performed after ion implantation was at  $600^\circ \text{ C}$ . However, significant differences arose in samples heat treated at  $900^\circ \text{ C}$ , namely in the STH matrix, as shown in Figures 1 and 2. In fact, STHB sample (heat treated at  $900^\circ \text{ C}$ ) presents the first and second shells (especially the second one) shifted to longer distances, when compared to STHA, silica-titania and silica-hafnia samples, suggesting a more open structure with either a) Si as second neighbor, (b) a different 2<sup>nd</sup> neighbor, such as Hf or, (c) eventually, a combination of Si and Hf, of the same type as the reported for  $\text{SiO}_2$  and  $\text{Al}_2\text{O}_3$  in reference [8]. For instance, second shell parameters are CN~6.12,  $r \sim 3.600 \text{ \AA}$  and  $\sigma \sim 0.029$ , for STHA and CN~6.28,  $r \sim 3.654 \text{ \AA}$ ,  $\sigma \sim 0.016$  for STHB. It should be noted also that the 2<sup>nd</sup> shell region appears more well-defined and intense for sample STHB, which might suggest that the Er environment is more crystallized, more ordered, for this sample, when compared to sample STHA. Moreover, STHA seems to present an intermediate behavior, in terms of bonding distance, between STB or SH900B and STHB, as shown in Table 1.
5. Heat treatment in SH900 samples also seems to have a minor influence in the Er environment, since the first shell becomes more intense with the heat treatment at  $900^\circ \text{ C}$  (sample SH900B), which means higher Er-O coordination number (or lower structural disorder), whereas in the second shell this does not occur. In silica-titania matrices, two  $\text{Er}^{3+}$  ions are likely to be bridged by a  $\text{SiO}_4$  tetrahedron and, therefore, the increase in oxygen coordination number corresponds to an increase in CN of Si [4]. However, in  $\text{SiO}_2\text{-HfO}_2$  samples the intensity of the second shell is not correlated with that of the first shell. This behavior could be related with the presence of Hf, that is known to disrupt the  $\text{SiO}_2$  network [10].
6. Sol-gel derived samples, where Ag and/or Er were incorporated by pore-doping (A10, with Er and A11, with Er and Ag), seem to exhibit a quite different radial-distribution of neighbors, as Figure 3 shows. However, such differences are not well depicted at the representation in K space, which brings some doubts to the previous observation. These samples have to be carefully studied, by repeating EXAFS analyses and/or by using other fitting programs. It should be noted that such a different environment around Er ions might explain the quite different photoluminescence peak shape in samples A10 and A11 at  $1.5 \text{ \mu m}$ , namely the much lower FWHM observed in sample A11 ( $\sim 24 \text{ nm}$ ), when compared to sample A10 ( $\sim 33 \text{ nm}$ ).

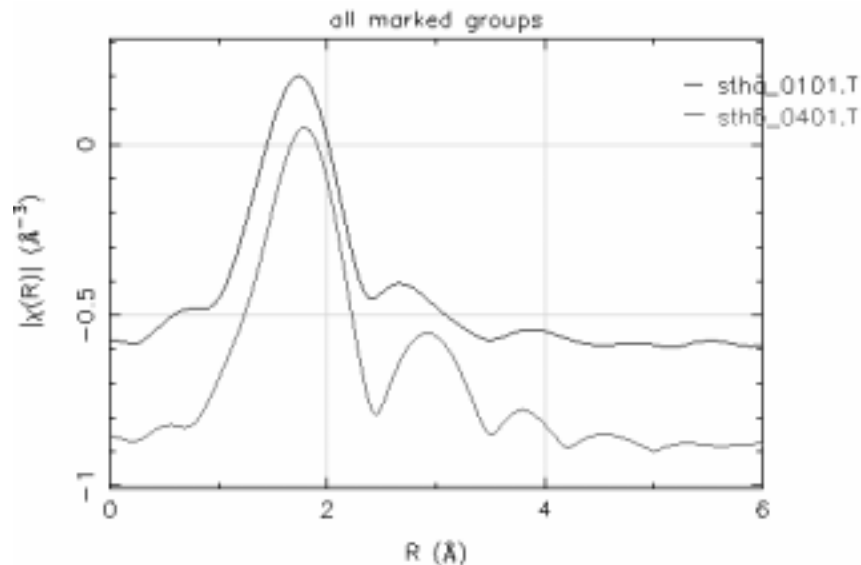


Figure 1

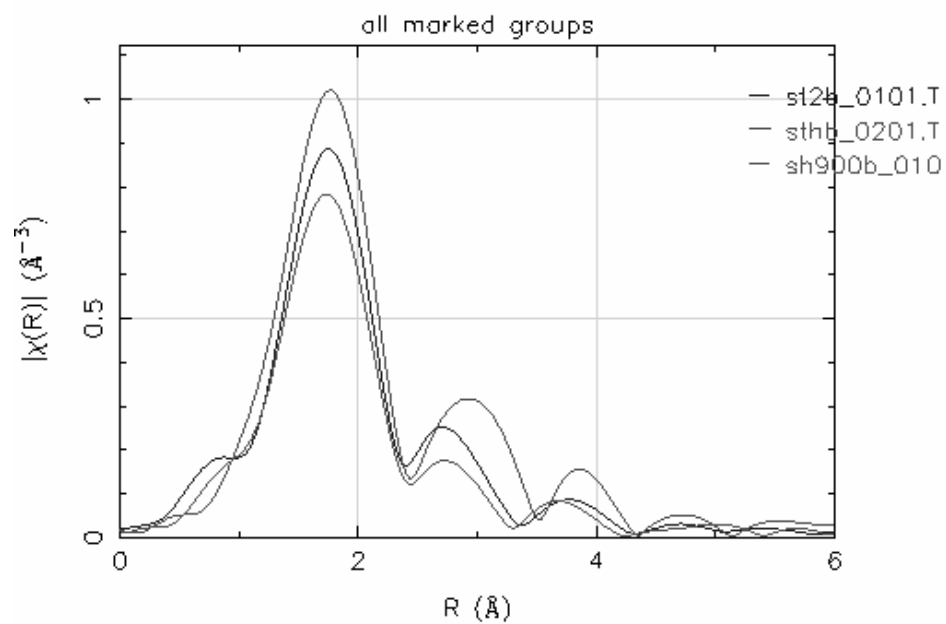


Figure 2

Table 1.

Sample	CN_O [±1]	r_O [±0.02]	ss_O [±0.004]	r_Si [±0.05]	ss_Si [±0.008]	E <sub>0</sub> [±2]
STA	6.26	2.27	0.0120	3.571	0.0186	5.14
STB	6.21	2.269	0.0144	3.586	0.0234	5.90
SH900A	5.88	2.269	0.0177	3.623	0.0281	5.33
SH900B	5.97	2.271	0.0152	3.591	0.0315	4.56
STHA	6.12	2.269	0.0159	3.600	0.0293	5.16
STHB	6.28	2.293	0.0124	3.654	0.0158	6.36

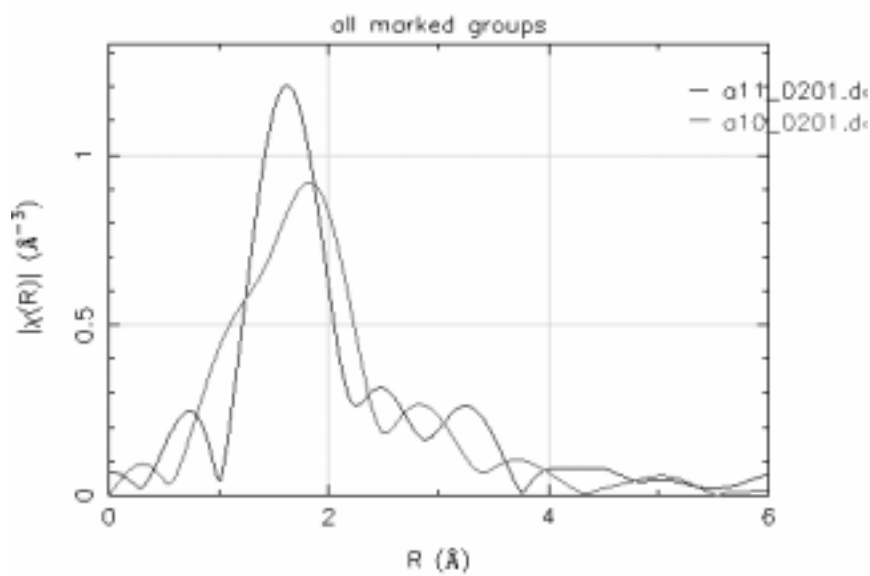


Figure 3